



Elevated nano- α -Fe₂O₃ enhances arsenic metabolism and dissolved organic carbon release of *Microcystis aeruginosa* under a phytate environment

Yinchai Luo^{1,2} · Jieru Zheng² · Qiuyao Ren² · Zhenhong Wang³ · Fen Huang¹ · Zixi Liu² · Zhuanxi Luo^{1,2} 

Received: 12 April 2023 / Accepted: 3 July 2023 / Published online: 10 July 2023
© The Author(s), under exclusive licence to Springer-Verlag GmbH Germany, part of Springer Nature 2023

Abstract

Little information is available on the effects of nano- α -Fe₂O₃ on arsenic (As) metabolism of algae and potential associated carbon (C) storage in As-contaminated water with dissolved organic phosphorus (DOP) as a phosphorus (P) source. In this study, *Microcystis aeruginosa* (*M. aeruginosa*) was used to investigate impacts of nano- α -Fe₂O₃ on cell growth and As metabolism of algae under a phytate (PA) environment as well as potential associated C storage. Results showed that nano- α -Fe₂O₃ had a subtle influence on algal cell growth in a PA environment. Herein, algal cell density (OD₆₈₀) and chlorophyll *a* (Chl*a*) were inhibited at elevated nano- α -Fe₂O₃ levels, which simultaneously limited the decrease of Yield. As suggested, the complexation of PA with nano- α -Fe₂O₃ could alleviate the negative influence on algal cell growth. Furthermore, the elevated nano- α -Fe₂O₃ increased As methylation in the PA environment due to higher monomethylarsenic (MMA) and dimethylarsenic (DMA) concentrations in the test media. Additionally, microcystins (MCs) in the media changed consistently with UV₂₅₄, both of which were relatively lower at 10.0 mg·L⁻¹ nano- α -Fe₂O₃. Enhanced As(V) methylation of algal cells was found to simultaneously reduce the release risk of As(III) and MC while increasing dissolved organic carbon (DOC) content in media, suggesting unfavorable C storage. Three-dimensional fluorescence analysis revealed that the main DOC constituent was the tryptophan-like component in aromatic proteins. Correlation analysis showed that decreases in pH and the zeta potential and an increase in Chl*a* may lead to metabolic As improvements in *M. aeruginosa*. The obtained findings highlight the need for greater focus on the potential risks of DOP combined with nano- α -Fe₂O₃ on algal blooms as well as the biogeochemical cycling processes of As and C storage in As-contaminated water with DOP as the P source.

Keywords Phytate · *Microcystis aeruginosa* · Arsenic species · Carbon storage

Responsible Editor: Gangrong Shi

✉ Zhuanxi Luo
zxluo@hqu.edu.cn

¹ Key Laboratory of Karst Dynamics, Ministry of Natural Resources (MNR) and Guangxi, Institute of Karst Geology, CAGS, Guilin 541004, China

² College of Chemical Engineering, Huaqiao University, Xiamen 361021, China

³ College of Chemistry, Chemical Engineering and Environment, Minnan Normal University, Key Laboratory of Modern Separation and Analysis Science and Technology, Key Laboratory of Pollution Monitoring and Control, Zhangzhou 363000, China

Introduction

The widespread application of nano- α -Fe₂O₃ leads to its inevitable release into the surrounding water environment, subsequently leading to corresponding eco-environmental effects. Nanoparticles in water environments can undergo aggregation/condensation, redox reactions, dissolution, exchange between surface groups, and reactions with biological macromolecules, which in turn affect the transport, fate, and toxicity of nanoparticles in the environment (Maurer-Jones et al. 2013). Since nanoparticles can aggregate on the surface of microorganisms and cause light-shading effects, nano- α -Fe₂O₃ is considered to be toxic to some algal species (Toh et al. 2016). It has been shown that nano- α -Fe₂O₃ can significantly reduce the cell size of *Nannochloropsis* sp. and *Isochrysis* sp. (Demir et al. 2015).

Furthermore, eutrophication combined with arsenic (As) pollution is common in actual water environments, and nanoparticles have an important impact on the biotransformation of As and its biogeochemical cycle in water environments (Bakhat et al. 2022; Hussain et al. 2021). As one of the dominant algal species of cyanobacterial blooms in eutrophic waterbodies, *Microcystis aeruginosa* (*M. aeruginosa*) is better able to adapt to different phosphorus (P) and As forms (Ji et al. 2017; Wang et al. 2019). Metabolic As mechanisms in microalgae can help mitigate As toxicity, specifically through reducing arsenate (As(V)) to arsenite (As(III)) and further methylating to organic arsenic forms (Bakhat et al. 2019; Che et al. 2018; Hussain et al. 2021). Moreover, studies have demonstrated that P forms in the environment affect As(V) tolerance, subsequently influencing biogeochemical As cycling processes (Bakhat et al. 2017; Leong and Chang 2020; Wang et al. 2019). It has been shown that *M. aeruginosa* can utilize nano- α -Fe₂O₃ for purposes of proliferation. Meanwhile, nano- α -Fe₂O₃, formed with bidentate and polynuclear, can complex with As(V) and phosphate (Fendorf and Kocar 2009), thus restricting As and P migration, which subsequently impacts As metabolism in algae (Luo et al. 2018).

Nano- α -Fe₂O₃ is widely recognized as having little impact on algae growth under a dissolved inorganic phosphorus (DIP) environment. However, its potential toxic effect is still unclear under a dissolved organic phosphorus (DOP) environment (Chen et al. 2022; Lei et al. 2016). Given that the proportion of DOP content is increasing in total dissolved P under current aquatic environmental conditions, it is critical to understand the impact of nano- α -Fe₂O₃ on algae growth as well as its specific metabolic As processes under a DOP environment. Phytate (PA) is widely considered the most abundant organic P species in soil and sediment, being freely available when released by algae (Bell et al. 2020; Yan et al. 2012). Meanwhile, a recent study demonstrated that phytate-P uptake stimulated *P. vittata* growth and As hyperaccumulation (Han et al. 2023), indicating that PA can potentially influence As metabolism in algae. Additionally, microalgal culture development used for carbon (C) capture and utilization demonstrates its potential contribution in addressing climate change challenges (Nguyen et al. 2023). However, there is little available information on the effects of nano- α -Fe₂O₃ on metabolic As processes in algae and C storage in As-contaminated water with DOP as a P source. Therefore, it has been hypothesized that level changes in nano- α -Fe₂O₃ may impact As metabolic processes in *M. aeruginosa* and even potential C storage in As-contaminated water with PA as a P source.

Accordingly, the aims of this study were to explore the effects of nano- α -Fe₂O₃ on the growth of *M. aeruginosa* under a PA environment, to investigate its metabolic accumulation of As(V) and variation of microcystin (MCs), and

to further observe dissolved organic carbon (DOC) changes combined with spectral analysis technologies, such as Fourier Transform Infrared Spectroscopy (FTIR) and 3D fluorescence analysis (3D-EEM), which can be used to identify the potential C storage under this experimental system. Findings from this study can enhance our understanding of the coexistence of nano- α -Fe₂O₃ and DOP on As biogeochemical cycling respective to algal mediation, which will help us to recognize ecological environmental risks under actual As-containing water bloom conditions.

Materials and methods

Algal species culture and pretreatment

Microcystis aeruginosa-905 specimens (purchased from the National Freshwater Algal Library of the Institute of Hydrobiology, Chinese Academy of Sciences) were cultured in a BG11 medium at 25 °C for 16 h: 8 h under a 3000 lx light intensity, shaken three times each day. Commercial nano- α -Fe₂O₃ (99.5%, 30 nm) and PA (CAS No. 83-86-3) were bought from Macklin Inc. (Shanghai, China). Before use, the nano- α -Fe₂O₃ specimens were immediately dispersed with sterilized ultrapure water for 1 h using an ultrasonic cell crusher (50 W/L, 40 kHz) in an ice bath, while Na₃AsO₄·12H₂O was prepared with an As(V) stock solution of 100 mg/L. During the logarithmic growth phase, algal specimens were separated through centrifugation at 4000 r/min and then placed in a Fe- and P-free modified BG11 medium (starvation culture) for 72 h so that the algal cells could adjust to this Fe and P deficient state.

Effects of nano- α -Fe₂O₃ on algal cell growth and arsenic metabolism

Under this Fe- and P-free state, *M. aeruginosa* cells were centrifuged and washed twice with sterile deionized water and then incubated in a modified BG11 medium with PA and nano- α -Fe₂O₃ for 96 h, at an initial PA concentration of 1.0 mg P/L, an initial As(V) concentration of 130 μ g As/L, and an initial nano-Fe₂O₃ concentration of 0.5, 1.0, 10.0, and 100 mg/L. The initial cell density was approximately 1.0×10⁷ cells/mL. Three parallel replicants were established for each abovementioned treatment, and all nano- α -Fe₂O₃ solutions without algae were used as blank controls. This method allowed us to compare the effects of nano- α -Fe₂O₃ on algal cell growth and As metabolism at low (0.5 and 1.0 mg/L) and elevated levels (10.0 and 100 mg/L) as well as their potential carbon storage under a PA environment. After sampling at 24 h intervals, chlorophyll *a* (Chl_a), actual photosynthetic yields (Yield), and algal cell density (OD₆₈₀) were determined as well as the pH, redox potential (ORP), and zeta potential in the algal solution. Meanwhile,

after 96 h of culturing, the algal solutions were centrifuged at 4000 r/min for 10 min. Afterward, the supernatant was filtered (0.22 μm , glass fiber membrane, Amicom) to determine MC, UV₂₅₄, DOC, FTIR, 3D-EEM, and As species. Moreover, the obtained algal cells were washed twice with deionized water to remove extracellular adsorbed nano- $\alpha\text{-Fe}_2\text{O}_3$ and As. Following this, they were stored at -20°C to determine total As (TAs) and their specific species according to our previously reported methods (Wang et al. 2019), briefly described below.

Analytical methods

Growth and medium environmental changes of *M. aeruginosa*

A fresh algal solution (3 mL) was used to measure OD₆₈₀ employing a UV spectrophotometer at a 680 nm wavelength. Meanwhile, after 10 min dark adaptation, approximately 2 mL of the fresh algal solution was detected for Chl *a* and Yield using an advanced phytoplankton plant fluorometer (PHYTO-PAM, Walz, Germany). Additionally, 5 mL of the algal solution was tested for its pH level, ORP, and zeta potential (Darwin, Zeta potential analyzer, England).

M. aeruginosa metabolites

According to a previously reported method (Zhou et al. 2020), MC content was determined using high-performance liquid chromatography (HPLC) on a C18 column at a 238 nm wavelength, with a flow rate of 1 mL/min and the mobile phase consisting of 0.1% trifluoroacetic acid and methanol (35:65). In the medium, DOC was measured using a total organic carbon analyzer (TOCV-CPH, Shimadzu, Japan) and UV₂₅₄ was detected using a UV visible spectrophotometer (Type MAPADA 722S, China) at a wavelength of 254 nm. The filtered supernatant was used to perform FTIR (Thermo Nicolet iS 10) observations with ultrapure water as the background. The spectra were recorded at intervals of 2 cm^{-1} at a spectral resolution of 4 cm^{-1} , 4000–500 cm^{-1} with 16 scans.

Moreover, using a fluorescence spectrophotometer (Varian Cary Eclipse) with ultrapure water as the background, 3D-EEM was used to determine dissolved organic matter (DOM) in the supernatant (Hasegawa et al. 2010; Wang et al. 2016a; Wang et al. 2022; Ziegmann et al. 2010). Specific scanning conditions were performed with an excitation wavelength (Ex) of 200–450 nm, a scan distance of 10 nm, and an emission wavelength (Em) of 250–550 nm (5 nm). The slit ratio was 10:10, and the scan speed was 1200 nm/min. Furthermore, the DOMFluor tool kit in MATLAB was utilized to perform 3D fluorescence data analysis with a parallel factor (PARAFAC). Ultrapure water data were removed from 3D-EEM results to avoid potential Raman scattering noise. Three component models that successfully

passed residual analysis, the split-half test, random initialization analysis, and the Tucker's congruence coefficient (TCC) test were considered reliable (Ly et al. 2019).

Arsenic species

The As species in the media and algae were pretreated according to our previous method (Wang et al. 2013) and measured using a HPLC-Inductively Coupled Plasma Mass Spectrometry (HPLC-ICP-MS, Agilent 7700) to determine the four As species, including As(V), As(III), monomethylarsenic (MMA), and dimethylarsenic (DMA). Specifically, the Agilent Company's PRP-X100 (250 \times 4.1 mm) type anion exchange column was used as the separation column at a mobile phase of 10 mM ammonium nitrate and 10 mM hydrogen phosphate with a pH level of 6.2 and a flow rate of 1 mL/min.

Data analysis

Our metabolic analysis of As(V) in *M. aeruginosa* is based on the As(V) metabolic mechanism of microalgae, in which cells absorb As(V), reduce to As(III), and then methylate As(III) to generate MMA and DMA (Hussain et al. 2021; Miyashita et al. 2016). Each biotransformation step involves both As accumulation and excretion processes. The total amount of As(V) metabolism and the accumulation and excretion rate of different As species in algal cells (fg/cell) were calculated according to a previously reported method (Che et al. 2018). Additionally, experimental results were shown as averaged values from three parallel (replicant) data with standard deviations and then graphed using Origin 2019 and GraphPad Prism 8.0. At the same time, one-way analysis of variance (ANOVA) was adopted to analyze the obtained data within and among the nano- $\alpha\text{-Fe}_2\text{O}_3$ treatments to evaluate the effects of the nano- $\alpha\text{-Fe}_2\text{O}_3$ on the study parameters of the selected data (significant level at $P < 0.05$). Furthermore, Pearson correlation analysis was also performed among the algal metabolites to understand their potential influencing mechanisms of As metabolism at the significant level of $P < 0.05$. The data were analyzed using SPSS statistical software (ver. 22) (SPSS Inc., Chicago, IL, USA).

Results and discussion

Growth and medium environmental changes of *M. aeruginosa*

The effects of different nano- $\alpha\text{-Fe}_2\text{O}_3$ concentrations on *M. aeruginosa* growth are shown in Fig. 1. Algal OD₆₈₀ increased over time (within 96 h) under the 10.0 mg/L

nano- α -Fe₂O₃ treatment, except that all showed a decreasing trend on the 4th day, especially the 100.0 mg/L nano- α -Fe₂O₃ treatment on the 3rd day ($P < 0.05$). Moreover, no significant differences were observed between the various treatments in the first 2 days (Fig. 1a). Changes in Chla (Fig. 1b) confirmed that there were no significant differences under the 1.0 mg/L nano- α -Fe₂O₃ treatment over time. By contrast, the remaining treatments showed a significant decreasing trend on the 3rd day, especially for the 10.0 and 100.0 mg/L nano- α -Fe₂O₃ treatments. This could potentially be due to conditions of oxidative reaction stress, which could have been induced by elevated nano- α -Fe₂O₃ concentrations that effectively disrupted the chloroplast structure (Lei et al. 2016; Saxena and Sangela 2020; Semerad et al. 2019; Toh et al. 2016). On the other hand, the elevated agglomerated nano- α -Fe₂O₃ concentration could have caused a shading effect to occur on the algal surface, which also can affect, to some extent, chlorophyll synthesis (Wang et al. 2013). According to Yield changes in algal cells (Fig. 1c), Yield in the nano- α -Fe₂O₃ 0.5 and 1.0 mg/L treatments significantly decreased on the 4th day, (i.e., only approx. 40% Yield compared to initial values). In contrast, Yield of the 10.0 and 100.0 mg/L nano- α -Fe₂O₃ treatments was still higher, indicating that

nano- α -Fe₂O₃ can alleviate Yield decreases at higher concentrations under a potential Fe deficiency (Bakhat et al. 2017). Generally, nano- α -Fe₂O₃ exhibited a slight impact on algal cell growth under a PA environment. This would inhibit OD₆₈₀ and Chla as PA concentrations increased while simultaneously limiting Yield decreases. This differed from the negative correlation between *Selenastrum capricornutum* density and nano- α -Fe₂O₃ concentrations (Wang 2019). The potential reason is that as a phosphorus source (Zhu and Wakisaka 2020), when some PA components complex with nano-Fe₂O₃, the negative influence on algal cell growth can be mitigated (He et al. 2017).

An increasing pH level trend was observed in the media as algal cells continued to grow (Fig. 1d), increasing from 8.0 on the initial day (0 days) to 10.0 on the 1st day. Among these, pH levels of the 0.5 and 1.0 mg/L nano- α -Fe₂O₃ treatments significantly decreased on the 4th day (i.e., being close to the pH level on 0 days). Similarly, although pH levels of the 10.0 and 100.0 mg/L nano- α -Fe₂O₃ treatments decreased on the 4th day, they were still relatively higher than that on 0 days (Fig. 1d). This implied that the 10.0 and 100.0 mg/L nano- α -Fe₂O₃ treatments may act as a good buffer to any potential decreases within the medium environment. Additionally, a significant decrease in ORP (150 mV reduction) occurred on

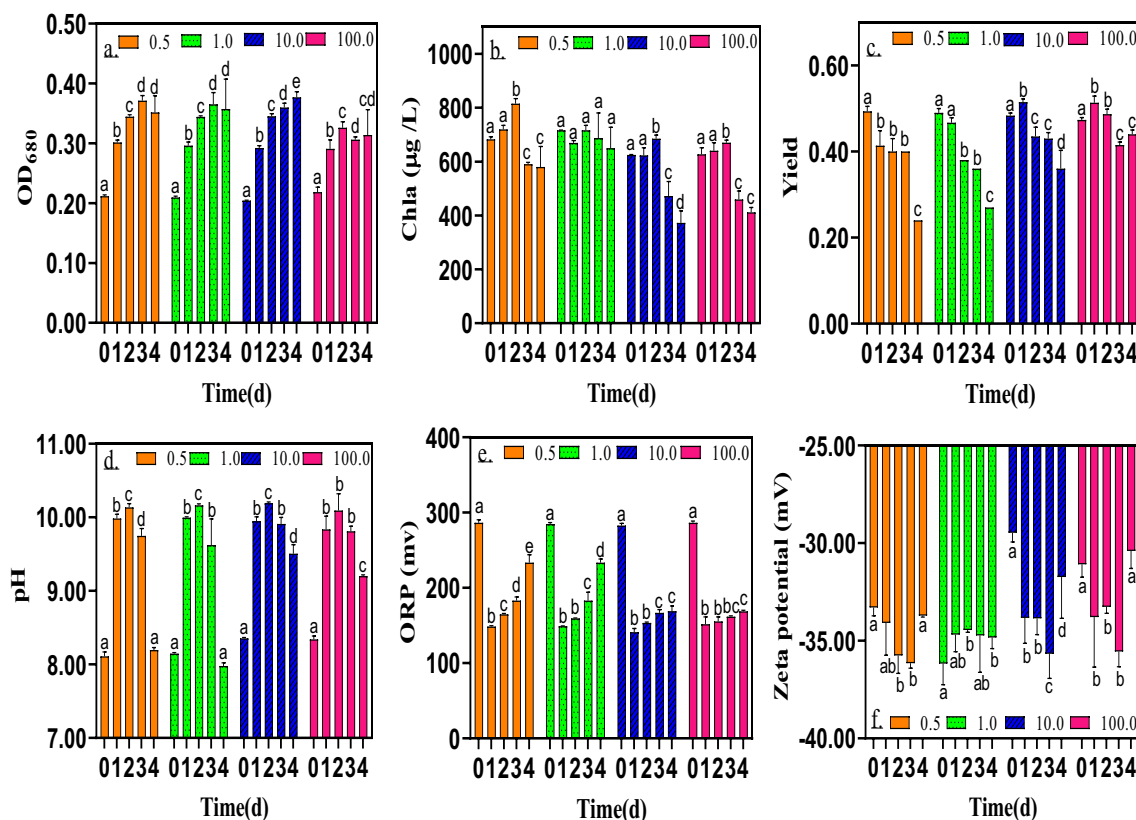


Fig. 1 Effects of nano- α -Fe₂O₃ (mg/L) on *Microcystis aeruginosa* growth and environmental conditions under a PA environment: **a** OD₆₈₀; **b** Chla; **c** Yield; **d** pH; **e** ORP; **f** zeta potential. Different letters indicate significant differences within nano- α -Fe₂O₃ treatments at a $P < 0.05$ level

the 1st day, after which a gradual ORP increase occurred over time in the 0.5 and 1.0 mg/L nano- α -Fe₂O₃ treatments. No obvious ORP shifts were observed in the 10.0 and 100.0 mg/L nano- α -Fe₂O₃ treatments (Fig. 1e). Furthermore, ORP and pH levels in the medium environment negatively correlated ($P < 0.001$), with a correlation coefficient of -0.970 . The higher nano- α -Fe₂O₃ concentration could apparently enhance pH and ORP in decreasing algal cell stability.

The zeta potential is an essential indicator used to describe the stability of colloidal dispersive systems in an aquatic environment, whose absolute value for a 25 mV system is commonly considered to be relatively stable (Tantra et al. 2010). The higher the absolute value is, the greater the electrostatic repulsion between particles will be and the better the physical stability of the aquatic environment. In this study, the absolute zeta potential value of the 1.0 mg/L nano- α -Fe₂O₃ treatment did not change significantly, while the other treatments first increased before gradually decreasing (Fig. 1f). Specifically, on the 4th day, the absolute zeta potential value of the 10.0 and 100.0 mg/L nano- α -Fe₂O₃ treatments decreased significantly, indicating that the addition of a higher nano- α -Fe₂O₃ concentration in the medium environment could reduce the particle stability of algal cells.

Arsenic metabolism

Arsenic species in algae and media

All nano- α -Fe₂O₃ treatments could detect As(V), DMA, MMA, and As(III), except for the 10.0 mg/L treatment without As(III) (Fig. 2a). Being a Fe source, nano- α -Fe₂O₃

did not change As(V) predominance within the PA environment media (Fig. 2a). The 100.0 mg/L nano- α -Fe₂O₃ treatment significantly decreased the As(V) concentration in the media ($P < 0.05$), showing higher As(V) removal. However, the 10.0 mg/L nano- α -Fe₂O₃ treatment effectively reduced As(III) concentrations in the media. This likely resulted from the appropriate oxidation condition produced or the inducement of ROS oxidative stress in algal cells via the nano- α -Fe₂O₃ additive (Lei et al. 2016). The higher DMA and MMA concentrations in the media under the PA environment indicated that nano- α -Fe₂O₃, as an Fe source, can promote As(V) methylation in algal cells under a PA environment. In contrast, nano-Fe₂O₃ in an inorganic P environment retarded the reduction of As(V) and then lessened the content of As methylation ($< 1.0 \mu\text{g/L}$) (Chen et al. 2022).

Moreover, total As (TAs) content in algae under the different nano- α -Fe₂O₃ treatments was relatively low (i.e., $6.37 \pm 1.80 \mu\text{g/g}$) (Fig. 2b). In particular, As(V) remained the dominant As species in algae, accounting for $72.3 \pm 5.2\%$ of the TAs (Fig. 2b). No significant differences in TAs were observed among treatments ($P > 0.05$). The lowest TAs observed in the 10.0 mg/L nano- α -Fe₂O₃ treatment was $4.36 \mu\text{g/g}$. Compared with As accumulation under an inorganic P environment, As accumulation under the PA environment significantly decreased (Chen et al. 2022). However, different nano- α -Fe₂O₃ concentrations had no significant impact on As accumulation and transformation (Fig. 2b). Specifically, PA exhibited a C-O-P organic complexing bond, which could effectively complex a large amount of As(V) under a PA environment and then interact with nano- α -Fe₂O₃ to form an As-Fe-DOM ternary complex (Zhang et al. 2020).

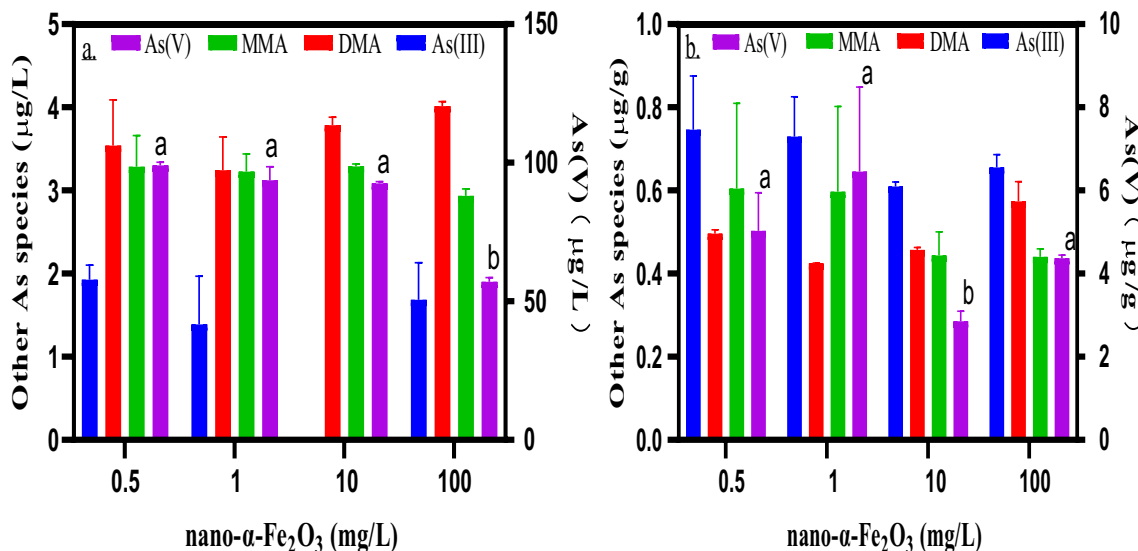
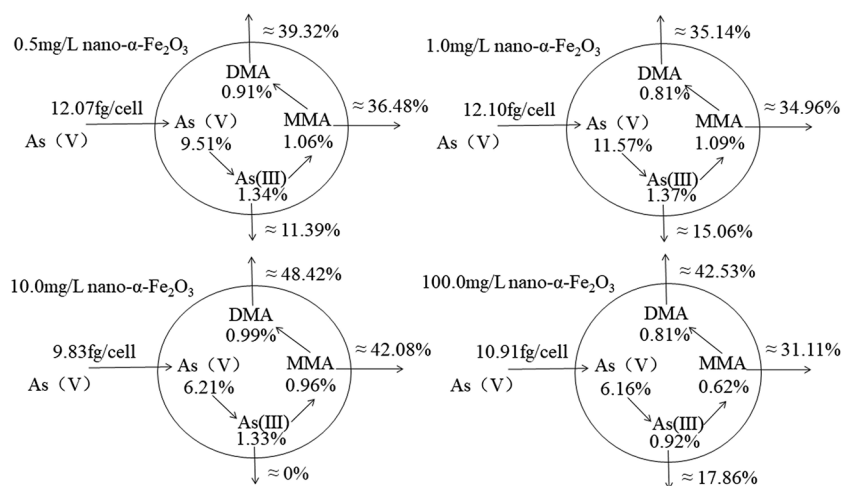


Fig. 2 Effects of nano- α -Fe₂O₃ on arsenic species under a PA environment: **a** medium; **b** algae. Different letters indicate significant differences among the different nano- α -Fe₂O₃ treatments at a $P < 0.05$

level. The same or no letters on bars indicate insignificant differences among different nano- α -Fe₂O₃ treatments at a $P < 0.05$ level

Fig. 3 Metabolic pathway of arsenic in *Microcystis aeruginosa* at different nano- α -Fe₂O₃ concentrations under a PA environment



This interaction could reduce As(V) uptake and accumulation by algal cells. Similarly, As(V) adsorption by nano- α -Fe₂O₃ in the media could also reduce As(V) accumulation (Luo et al. 2020). Meanwhile, the biotransformation of algal As under the PA environment was mainly regulated by PA phosphorus because PA is symmetrical and relatively stable so that the produced P deficiency promotes As biotransformation (Wang et al. 2019). Meanwhile, PA interactions with additive nano- α -Fe₂O₃ and As did not limit a reduction in As(V) in algae and subsequent methylation. Nevertheless, specific relevant mechanisms require further investigation.

Arsenic metabolism pathway

Results showed a slight decrease in total As(V) metabolism as nano- α -Fe₂O₃ concentrations increased (Fig. 3). The 10.0 mg/L nano- α -Fe₂O₃ treatment had the lowest total As(V) metabolic rate (i.e., 9.83 fg/cell) and the highest methylation total metabolic rate (i.e., 92.5%). The remaining nano- α -Fe₂O₃ treatments showed a relative inhibition on As(III) methylation (Fig. 3). As(V) metabolism under the PA environment was mainly caused by the extracellular excretion

of DMA and MMA, accounting for greater than 31.11% and 35.14% of the total metabolism, respectively (Fig. 3). This indicated that the PA environment could promote As methylation in algae. The PA molecule, as a strong ligand, which has six phosphate groups and a relatively elevated charge density (Chen and Arai 2019; Chen et al. 2020), could complex with nano- α -Fe₂O₃, subsequently reducing P bioavailability. Moreover, PA is relatively stable, indicating that it does not easily release inorganic P (Yan et al. 2012). Therefore, under P-limiting conditions, As(V) was absorbed by algal cells and reduced to As(III), while As(III) was further methylated into DMA and eventually this DMA secreted into the culture medium (Wang et al. 2015). Compared with the inorganic P environment at a low As(V) concentration (i.e., 15 μ g/L) (Che et al. 2018), the As metabolite of individual algae cells under an elevated initial As(V) concentration in this PA environment was greater by a factor of 10, while MMA release reached a factor of 6–8. This could have resulted from a P deficiency, the combined effect of external organic C sources, and Fe deficiency under the PA environment (Bakhat et al. 2017), which should be further investigated.

Fig. 4 Effects of the nano- α -Fe₂O₃ on MCs, UV₂₅₄, and DOC under a PA environment: **a** MCs and UV₂₅₄; **b** DOC. Different letters indicate significant differences among different nano- α -Fe₂O₃ treatments at a $P < 0.05$ level

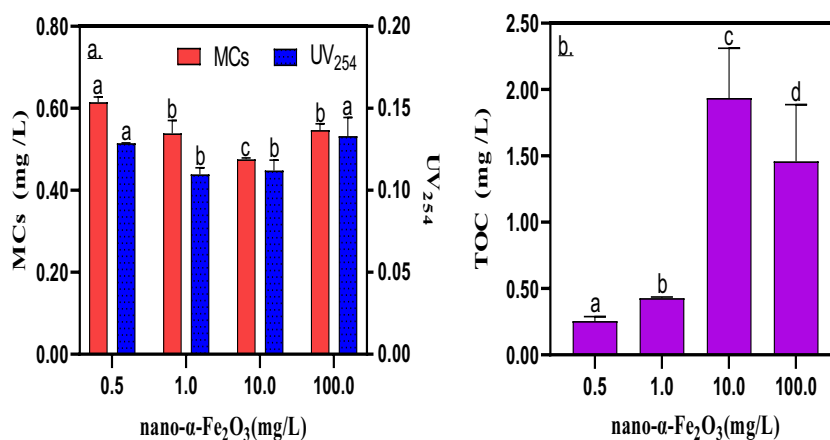
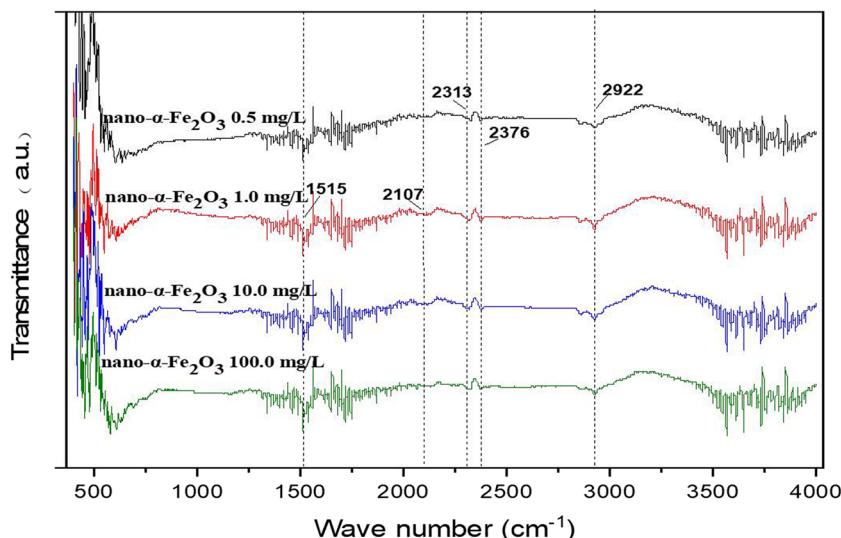


Fig. 5 IR spectra of DOM in PA media influenced by nano- α - Fe_2O_3



Furthermore, the total amount of As that metabolized in individual algal cells significantly and negatively correlated with OD_{680} , the pH level, the zeta potential, and Chl*a*, whose corresponding correlation coefficients were -0.958 , -0.951 , -0.933 , and 0.972 , respectively ($P < 0.05$). This demonstrated that the poorer the algae growth and the lower the algal density were, the higher the As metabolism presented. Concurrently, decreases in pH levels and zeta potentials and increases in Chl*a* content were also favorable to As metabolism. This was consistent with findings from previous studies that indicated that P was the main influencing factor of algal cell growth, and algal cell

growth restrictions could significantly promote As transformation (Che et al. 2018; Zhang et al. 2023).

Metabolites

MCs, UV_{254} and DOC

Both MCs and UV_{254} were U in shape with increasing nano- α - Fe_2O_3 concentrations (Fig. 4). The lowest MC content was observed in the 10.0 mg/L nano- α - Fe_2O_3 treatment (i.e., 0.47 mg/L); meanwhile, UV_{254} in both the 1.0 and 10.0 mg/L treatments markedly decreased ($P < 0.05$). Moreover, UV_{254}

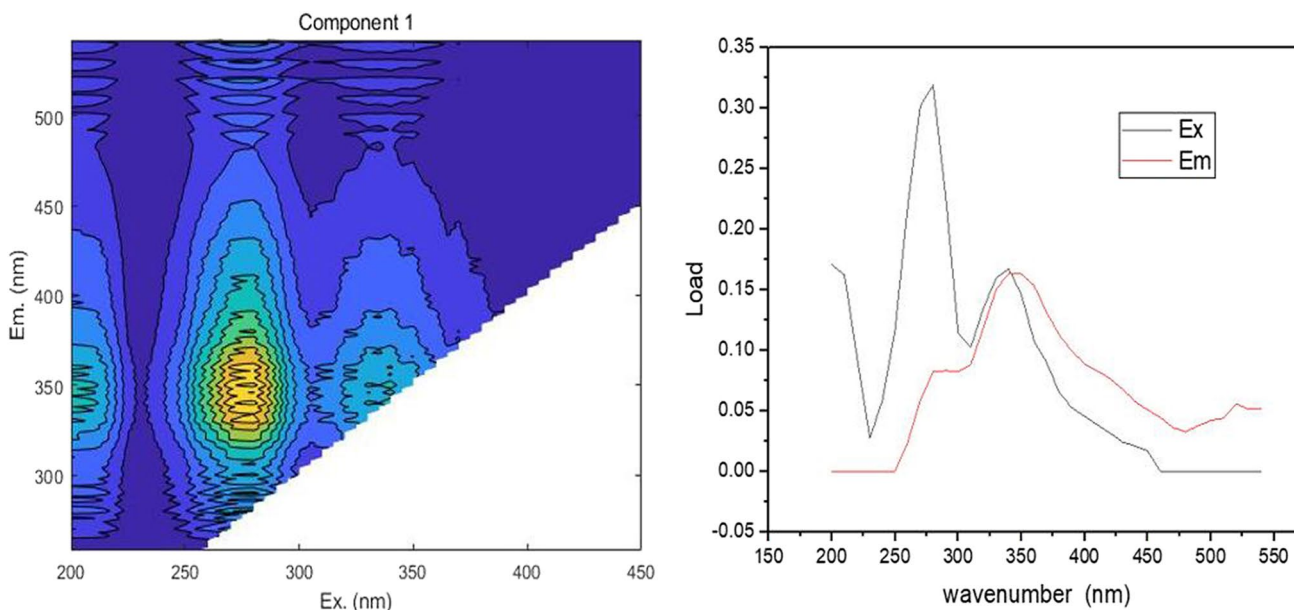


Fig. 6 Fluorescent fraction of DOM and its Ex-Em load at different nano- α - Fe_2O_3 concentrations under PA environment as determined by the PARAFAC method

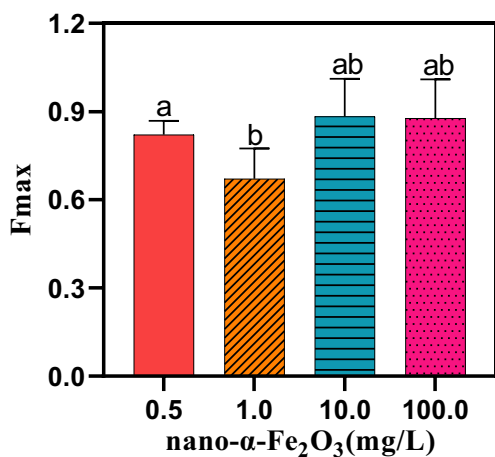


Fig. 7 Maximum fluorescence intensity of DOM under PA environment at different nano- α -Fe₂O₃ concentrations in the PARAFAC model. Different letters indicate significant differences among different nano- α -Fe₂O₃ treatments at $P < 0.05$

and MC significantly positively correlated, with a correlation coefficient of 0.638 ($P < 0.05$). As previously suggested, there was a suitable and effective nano- α -Fe₂O₃ concentration that could reduce UV₂₅₄ and MC content in media under the PA environment, thus mitigating organic contamination risks in the aquatic environment from algal cell proliferation. Potential reasons for this are algal cell and MC adsorption onto nano- α -Fe₂O₃, which can reduce MCs to some extent in aquatic environments. PA changed the permeability of the cell membrane. This could also inhibit MC and organic matter release (Wang et al. 2016b). Meanwhile, the increased release of MCs and UV₂₅₄ under elevated nano- α -Fe₂O₃ may be due to algal cell adsorption and its subsequent shading effect on algal cells under high nano- α -Fe₂O₃ concentrations, which stimulates the secretion of MCs and organic matter in algal cells to resist any effects of an adverse environment (Ouyang et al. 2015; Saxena and Sangela 2020; Siddiqui et al. 2021).

The DOC content in media tended to increase with increasing nano- α -Fe₂O₃ concentrations (Fig. 4b). The highest DOC content in the 10.0 mg/L nano- α -Fe₂O₃ treatment was 1.94 mg/L, indicating that the total amount of organic matter was higher in this treatment. In addition, DOC was negatively correlated with the total metabolism of Chla, ORP, and individual algal cell As content, with corresponding correlation coefficients of -0.845 , -0.891 , and -0.971 ($P < 0.05$), respectively. Meanwhile, DOC positively correlated with Yield, pH level, and zeta potential, with corresponding correlation coefficients of 0.758, 0.915, and 0.742 ($P < 0.05$), respectively. Therefore, conditions associated with a decrease in total Chla, ORP, and As metabolism by algal cells or increases in Yield, pH level, and zeta potential values can favor the release of organic matter from algal cells, thus contributing DOM to the environment, which is unfavorable to C storage (Kalokora et al. 2022; Nguyen et al. 2023).

FTIR and EEM analysis

Characteristic absorption peaks of the main functional group of organic matter in media were not affected by changes in nano- α -Fe₂O₃ concentrations (Fig. 5), which likely resulted from the relatively higher stability of the PA environment (Yan et al. 2012). Results showed that the main absorption feature peaked at 1515 cm⁻¹ with the -C-N expansion vibration representing the amide II band material in the protein, 2922 cm⁻¹ with -CH₃ anti-symmetrical stretching vibration representing protein and lipid sugars, 2376 and 2313 cm⁻¹ with CO₂ and HCO₃⁻ symmetrical stretching vibration representing carbonate matter, and 2107 cm⁻¹ with C≡C stretching vibration representing alkyne substances.

Furthermore, analysis of the EEM-PARAFAC model revealed that DOM in the media only exhibited one set of fluorescent components (Fig. 6), located at Ex/Em = 280/340 nm, showing a single maximum excitation and emission peak. This indicates the aromatic protein-like substance II (i.e., tryptophan-like substance) (Li et al. 2014). Previously, studies had shown that algae could secrete a large amount of extracellular organic matter to the surrounding environment at the beginning of its growth stage, manifested as tryptophan-like substance enhancements (Villacorte et al. 2015). From the maximum fluorescence intensity value (F_{max}), the 10.0 and 100.0 mg/L of the nano- α -Fe₂O₃ treatments had a relatively higher DOM concentration, while the 1.0 mg/L nano- α -Fe₂O₃ treatment exhibited a lower DOM level (Fig. 7). This implied that 1.0 mg/L nano- α -Fe₂O₃ could distinctly reduce the release of DOM into the media by *M. aeruginosa* under a PA environment. Moreover, F_{max} significantly correlated with both pH level and Chla ($P < 0.05$), with the correlation coefficient of 0.677 and -0.692 , respectively. This indicated that the DOM that was released was affected by the environmental pH and Chla. Specifically, algal cells could induce an increase in pH in media and mitigate Chla through DOM release.

Conclusions

In As(V) contaminated water under PA environment, nano- α -Fe₂O₃ had a slight impact on algal cell growth, inhibiting OD₆₈₀ and Chla with increasing concentrations while simultaneously limiting decreases in Yield. This indicated that as a phosphorus source, PA that complexed with nano-Fe₂O₃ could mitigate the negative influence on algal cell growth. Additionally, higher nano- α -Fe₂O₃ concentrations appear to apparently enhance pH levels and ORP to evidently reduce algal cell stability, supported by the significant decrease observed in the absolute zeta potential value. Furthermore, although As(V) remained the dominant As species in both algal specimens and the media, *M. aeruginosa* showed an elevated As methylation capacity under the PA environment in the higher nano- α -Fe₂O₃ treatment, which was supported by the higher DMA and MMA

concentrations in the media under the PA environment. Particularly, 100.0 mg/L nano- α -Fe₂O₃ can significantly reduce As risks in an aquatic environment due to the higher accumulation and methylation of As in algae as well as the adsorptive removal of As by nano- α -Fe₂O₃ from the media, while 10.0 mg/L nano- α -Fe₂O₃ effectively decreased As accumulation, the release of As(III), and subsequently As(V) metabolism in individual algae cells, ultimately promoting As(V) methylation by *M. aeruginosa*. Moreover, lower UV₂₅₄ and DOM values were observed in the 1.0 mg/L nano- α -Fe₂O₃ treatment, effectively reducing the organic matter released into the surrounding environment. Meanwhile, the 10.0 mg/L nano- α -Fe₂O₃ treatment had the lowest MCs and highest DOC content, demonstrating the effect of increased organic levels and a reduction in MC risk. Correlation analysis results showed that algal cells could induce an increase in pH in the media and mitigate Chla through DOM release, which, according to fluorescent analysis, is mainly composed of tryptophan-like substances. Moreover, a decrease in pH levels and zeta potentials and an increase in Chla content favored As metabolism but did not favor C storage. However, potentially relevant mechanisms are required for further investigations. Generally, it is critical to acquire a profound understanding on how nano- α -Fe₂O₃ influences algal blooms, As biotransformation processes, and potential C storage under a DOP environment.

Acknowledgements We would also like to acknowledge the anonymous reviewers and editors for their critical and helpful comments on the manuscript.

Author contribution All authors contributed to the study's conception and design. Material preparation, data collection, and analysis were performed by Yinchai Luo, Jieru Zheng, Qiuyao Ren, Zhenhong Wang, Fen Huang, Zixi Liu, and Zhuanxi Luo. The first draft of the manuscript was written by Yinchai Luo, Jieru Zheng, Qiuyao Ren, Zhenhong Wang, Fen Huang, and Zhuanxi Luo. All authors commented on previous versions of the manuscript. All authors read and approved the final manuscript.

Funding This study was supported by the Guangxi Key Science and Technology Innovation Base on Karst Dynamics, China (KDL & Guangxi 202011); the Project of Industry university cooperation in Fujian Province, China (2022N5002); and the Nature Science Foundation of China (42177384).

Data availability The datasets used during this study are available from the corresponding author on request.

Declarations

Ethics approval All the authors declare that the present research was organized by considering all ethical standards.

Consent to participate All authors shared equally in the preparation of this manuscript.

Consent for publication All authors approved the manuscript for publication.

Competing interests The authors declare no competing interests.

References

- Bakhat HF, Zia Z, Fahad S, Abbas S, Hammad HM, Shahzad AN, Abbas F, Alharby H, Shahid M (2017) Arsenic uptake, accumulation and toxicity in rice plants: possible remedies for its detoxification: A review. *Environ Sci Pollut R* 24:9142–9158
- Bakhat HF, Zia Z, Abbas S, Hammad HM, Shah GM, Khalid S, Shahid N, Sajjad M, Fahad S (2019) Factors controlling arsenic contamination and potential remediation measures in soil-plant systems. *Groundw for Sustain Dev* 9:100263
- Bakhat HF, Arshad S, Natasha AS, Shah GM, Fahad S, Hammad HM, Sajjad M, Ashfaq M, Shahid M (2022) Genotypic differences among the rice genotypes to arsenic stress cultivated under two water regimes: with an inference to human health. *J Plant Growth Regul* 41:558–568
- Bell DW, Pellechia PJ, Inga ED, Benitez-Nelson CR (2020) Resolving marine dissolved organic phosphorus (DOP) composition in a coastal estuary. *Limnol Oceanogr* 65:2787–2799
- Che F, Du M, Yan C (2018) Arsenate biotransformation by *Microcystis aeruginosa* under different nitrogen and phosphorus levels. *J Environ Sci* 66:41–49
- Chen A, Arai Y (2019) Functional group specific phytic acid adsorption at the ferrihydrite-water interface. *Environ Sci Technol* 53:8205–8215
- Chen A, Li Y, Shang J, Arai Y (2020) Ferrihydrite transformation impacted by coprecipitation of phytic acid. *Environ Sci Technol* 54:8837–8847
- Chen Y, Wang Z, Luo Z, Zhao Y, Yu J (2022) Decreasing arsenic accumulation but promoting arsenate biotransformation in *Microcystis aeruginosa* regulated by nano-Fe(2)O(3). *Environ Sci Pollut R* 29:62423–62431
- Demir V, Ates M, Arslan Z, Camas M, Celik F, Bogatu C, Can SS (2015) Influence of alpha and gamma-iron oxide nanoparticles on marine microalgae species. *Bull Environ Contam Toxicol* 95:752–757
- Fendorf S, Kocar BD (2009) Biogeochemical processes controlling the fate and transport of arsenic: implication for South and Southeast Asia. In: Sparks DL (Editor). *Adv Agron* 104:137–164
- Han R, Chen JY, He SX, Liu CJ, Dai ZH, Liu X, Cao Y, Ma LQ (2023) Phytate and arsenic enhance each other's uptake in *As-hyperaccumulator Pteris vittata*: root exudation of phytate and phytase, and plant uptake of phytate-P. *Environ Sci Technol* 57:190–200
- Hasegawa H, Rahman MA, Kitahara K, Itaya Y, Maki T, Ueda K (2010) Seasonal changes of arsenic speciation in lake waters in relation to eutrophication. *Sci Total Environ* 408:1684–1690
- He M, Yan Y, Pei F, Wu M, Gebreluel T, Zou S, Wang C (2017) Improvement on lipid production by *Scenedesmus obliquus* triggered by low dose exposure to nanoparticles. *Sci Rep* 7:15526
- Hussain MM, Wang J, Bibi I, Shahid M, Niazi NK, Iqbal J, Mian IA, Shaheen SM, Bashir S, Shah NS, Hina K, Rinklebe J (2021) Arsenic speciation and biotransformation pathways in the aquatic ecosystem: the significance of algae. *J Hazard Mater* 403:124027
- Ji N, Wang S, Zhang L (2017) Characteristics of dissolved organic phosphorus inputs to freshwater lakes: a case study of Lake Erhai, southwest China. *Sci Total Environ* 601:1544–1555
- Kalokora OJ, Gullstrom M, Buriyo AS, Mtolera MSP, Bjork M (2022) Seagrass meadows mixed with calcareous algae have higher plant productivity and sedimentary blue carbon storage. *Ecol Evol* 12:e8579
- Lei C, Zhang L, Yang K, Zhu L, Lin D (2016) Toxicity of iron-based nanoparticles to green algae: effects of particle size, crystal phase, oxidation state and environmental aging. *Environ Pollut* 218:505–512

- Leong YK, Chang JS (2020) Bioremediation of heavy metals using microalgae: recent advances and mechanisms. *Bioresour Technol* 303:122886
- Li W-T, Chen S-Y, Xu Z-X, Li Y, Shuang C-D, Li A-M (2014) Characterization of dissolved organic matter in municipal wastewater using fluorescence PARAFAC analysis and chromatography multi-excitation/emission scan: a comparative study. *Environ Sci Technol* 48:2603–2609
- Luo Z, Wang Z, Yan Y, Li J, Yan C, Xing B (2018) Titanium dioxide nanoparticles enhance inorganic arsenic bioavailability and methylation in two freshwater algae species. *Environ Pollut* 238:631–637
- Luo ZX, Wang ZH, Xing BS (2020) Insights into the uptake, distribution, and efflux of arsenite associated with nano-TiO₂ in determining its toxicity on *Daphnia magna*. *Environ Sci-Nano* 7:1194–1204
- Ly QV, Lee MH, Hur J (2019) Using fluorescence surrogates to track algogenic dissolved organic matter (AOM) during growth and coagulation/flocculation processes of green algae. *J Environ Sci* 79:311–320
- Maurer-Jones MA, Gunsolus IL, Murphy CJ, Haynes CL (2013) Toxicity of engineered nanoparticles in the environment. *Anal Chem* 85:3036–3049
- Miyashita S-i, Murota C, Kondo K, Fujiwara S, Tsuzuki M (2016) Arsenic metabolism in cyanobacteria. *Environ Chem* 13:577–589
- Nguyen LN, Vu MT, Vu HP, Johir MAH, Labeeuw L, Ralph PJ, Mahlia TMI, Pandey A, Sirohi R, Nghiem LD (2023) Microalgae-based carbon capture and utilization: a critical review on current system developments and biomass utilization. *Crit Rev Env Sci Tec* 53:216–238
- Ouyang S, Hu X, Zhou Q (2015) Envelopment-internalization synergistic effects and metabolic mechanisms of graphene oxide on single-cell *Chlorella vulgaris* are dependent on the nanomaterial particle size. *ACS Appl Mater Interfaces* 7:18104–18112
- Saxena P, Sangela V, Harish (2020) Toxicity evaluation of iron oxide nanoparticles and accumulation by microalgae *Coelastrella ter-restris*. *Environ Sci Pollut R* 27:19650–19660
- Semerad J, Moeder M, Filip J, Pivokonsky M, Filipova A, Cajthaml T (2019) Oxidative stress in microbes after exposure to iron nanoparticles: analysis of aldehydes as oxidative damage products of lipids and proteins. *Environ Sci Pollut R* 26:33670–33682
- Siddiqui MH, Alamri S, Mukherjee S, Al-Amri AA, Alsubaie QD, Al-Munqedhi BMA, Ali HM, Kalaji HM, Fahad S, Rajput VD, Narayan OP (2021) Molybdenum and hydrogen sulfide synergistically mitigate arsenic toxicity by modulating defense system, nitrogen and cysteine assimilation in faba bean (*Vicia faba* L.) seedlings. *Environ Pollut* 290:117953
- Tantra R, Schulze P, Quincey P (2010) Effect of nanoparticle concentration on zeta-potential measurement results and reproducibility. *Particuology* 8:279–285
- Toh PY, Tai WY, Ahmad AL, Lim JK, Chan DJC (2016) Toxicity of bare and surfaced functionalized iron oxide nanoparticles towards microalgae. *Int J Phytoremediat* 18:643–650
- Villacorte LO, Ekowati Y, Neu TR, Kleijn JM, Winters H, Amy G, Schippers JC, Kennedy MD (2015) Characterisation of algal organic matter produced by bloom-forming marine and freshwater algae. *Water Res* 73:216–230
- Wang C, Wang X, Wang P, Chen B, Hou J, Qian J, Yang Y (2016a) Effects of iron on growth, antioxidant enzyme activity, bound extracellular polymeric substances and microcystin production of *Microcystis aeruginosa* FACHB-905. *Ecotoxicol Environ Saf* 132:231–239
- Wang H, Qu G, Gan Y, Zhang Z, Li R, Wang T (2022) Elimination of *Microcystis aeruginosa* in water via dielectric barrier discharge plasma: efficacy, mechanism and toxin release. *J Hazard Mater* 422:126956
- Wang Y, Wang S, Xu P, Liu C, Liu M, Wang Y, Wang C, Zhang C, Ge Y (2015) Review of arsenic speciation, toxicity and metabolism in microalgae. *Rev Environ Sci Bio* 14:427–451
- Wang Y, Zheng Y, Liu C, Xu P, Li H, Lin Q, Zhang C, Ge Y (2016b) Arsenate toxicity and metabolism in the halotolerant microalga *Dunaliella salina* under various phosphate regimes. *Environ Sci-Proc Imp* 18:735–743
- Wang YX (2019) Study on toxic effects of nano Fe₂O₃ and tetracycline on *Selenastrum capricornutum*. Hebei University of Science and Technology In Chinese
- Wang Z, Luo Z, Yan C (2013) Accumulation, transformation, and release of inorganic arsenic by the freshwater cyanobacterium *Microcystis aeruginosa*. *Environ Sci Pollut R* 20(10):7286–7295
- Wang Z, Gui H, Luo Z, Zhen Z, Yan C, Xing B (2019) Dissolved organic phosphorus enhances arsenate bioaccumulation and biotransformation in *Microcystis aeruginosa*. *Environ Pollut* 252:1755–1763
- Yan Y, Wan B, Liu F, Tan W, Liu M, Feng X (2012) Distribution, species and interfacial reactions of phytic acid in environment. *Chinese J Appl Environ Biol* 18:494–501
- Zhang J, Zhou F, Liu Y, Huang F, Zhang C (2020) Effect of extracellular polymeric substances on arsenic accumulation in *Chlorella pyrenoidosa*. *Sci Total Environ* 704:135368
- Zhang X, Wang Z, Luo Z, Chen Y, Huang X (2023) Insights into the conversion of dissolved organic phosphorus favors algal bloom, arsenate biotransformation and microcystins release of *Microcystis aeruginosa*. *J Environ Sci* 125:205–214
- Zhou Y, Li X, Xia Q, Dai R (2020) Transcriptomic survey on the microcystins production and growth of *Microcystis aeruginosa* under nitrogen starvation. *Sci Total Environ* 700:134501
- Zhu J, Wakisaka M (2020) Finding of phytase: understanding growth promotion mechanism of phytic acid to freshwater microalga *Euglena gracilis*. *Bioresour Technol* 296:122343
- Ziegmann M, Abert M, Mueller M, Frimmel FH (2010) Use of fluorescence fingerprints for the estimation of bloom formation and toxin production of *Microcystis aeruginosa*. *Water Res* 44:195–204

Publisher's note Springer Nature remains neutral with regard to jurisdictional claims in published maps and institutional affiliations.

Springer Nature or its licensor (e.g. a society or other partner) holds exclusive rights to this article under a publishing agreement with the author(s) or other rightsholder(s); author self-archiving of the accepted manuscript version of this article is solely governed by the terms of such publishing agreement and applicable law.